

Modeling the Solar Limb Brightening at 21 cm Using Amplitude and Closure Phase Measurements from a 3-Element Interferometer.

J.K. Oiler

University of Wisconsin, Madison, WI, 53706

A.E.E. Rogers

and Divya Oberoi

MIT Haystack Observatory, Westford, MA 01886

(E-mail: arogers@haystack.mit.edu)

Abstract. Measurements of the interferometric amplitude and closure phase from a 3-baseline interferometer were used to model the Sun's radio image at 21 cm wavelength. The data were obtained from 9 June through 7 August 2006. During this period the solar activity was relatively quiet and the data is well fit using a model of equatorial limb brightening which contributes 30 ± 10 percent of the total solar radio flux. Modeling the image with circularly symmetric brightening or polar limb brightening does not fit the measurements making the result clear evidence that the limb brightening is largely equatorial.

During the period of the observations the days with asymmetric modeled images, as indicated by values of the closure phase which deviate from zero or 180 degrees, are well fit by adding from a single sunspot whose best fit position is consistent with the position of the major sunspot in the optical image for that day.

Key words: Sun: corona, radio radiation, instrumentation; interferometers

1. Introduction

We set-up a small interferometer at Haystack Observatory, Westford, Massachusetts (42.5N, 71.5W) using three 2.3 m parabolic dishes in a small triangle, with the longest baseline of about 25 m. Each dish and its associated electronics were independent small radio telescopes (SRTs) whose local oscillators and data sampling are controlled by GPS thereby allowing

interferometry in a “VLBI mode”. The dishes were programmed to track the sun and record to disk ten seconds of one-bit-sampled data with 4 MHz bandwidth at a 8 Ms/s rate every 10 minutes. The observing band was centered at 1417 MHz. At the end of each day the data files were retrieved and correlated in custom software by another PC. Figure 1 shows the 3 SRT interferometer. The SRTs, labeled SRT1, SRT2 and SRT3 were placed so that SRT3 was 26.67 m from SRT2 along an azimuth of 322 degrees and SRT1 was 7.77 m from SRT2 along an azimuth of 351 degrees. The 3-baseline data were correlated and the normalized correlation and phases calculated for each coherent integration period of 0.512 s. The closure phase was then calculated from the phases on each of the 3-baselines and the normalized correlations were corrected for the system noise to form the normalized visibilities which have a value of one if the Sun is unresolved.

2. Solar image modeling

The Sun’s radio image was modeled using weighted least squares to minimize, Q , chi-squared for N observations on each day where

$$Q = \sum_j \sum_i (m_{ij} - a_{ij})^2 + \sum_j (\cos(mc_j) - \cos(c_j))^2 + \sum_j (\sin(mc_j) - \sin(c_j))^2 \quad (1)$$

and m_{ij} = model amplitudes

a_{ij} = observed amplitudes

mc_j = model closure phases

c_j = observed closure phases

i = baseline index, 0 to 2

j = time index, 0 to $N-1$.

The quality of the fit was determined from the rms residual $(Q/5N)^{1/2}$. First, the very simple model of a uniform circular disk with the optical radius was found to be a poor fit. Next, we added some circularly symmetric limb brightening and found no improvement. Acceptable fits required the limb brightening to be restricted to the equatorial zone and on some days we had to add a single point

source representing a “sunspot” to the model to obtain a good fit. The closure phase is especially sensitive to asymmetries in the image as a symmetrical image can only result in closure phase values of 0 or 180 degrees. Because the modeling is highly non-linear we used a 4 dimensional search to determine the following parameters:

1] A global parameter for all days representing the fraction of the total solar flux density in the equatorial limb brightening.

2] The 2-D position along with the fractional strength of an unresolved sunspot on the solar disk.

In the geometrical calculations of the projected baselines in the direction of the Sun we accounted for the apparent tilt of the solar rotation axis, known as the position angle of axis p , relative to the direction of increasing declination. Apart from the tilt correction we left our images with the apparent projected view of the Sun since the heliographic latitude in the direction of Earth was less than about 5 degrees for the period of the observations.

As an example, Figure 2 shows the model fit for day number of the year 189 (8 July 2006) along with the model image for that day. Figure 3 shows the sequence of model images from day 160 through 219. Some days were missed owing to various problems with one of the SRTs. For some periods the modeled sunspot appears to move across the solar disk with a location approximately consistent with the largest sunspot in the optical image for that day. The uv coverage with 3 baselines was not sufficient to include more than one sunspot in the modeling even though there may have been more than one sunspot in the optical image. However, there were seldom more than one sunspot in the optical image for the period of the observations.

3. Results and discussion

With the very limited uv coverage of the 3 baselines we found the simplest model consistent with our data to be a uniform disk with equatorial limb brightening with an excess fractional flux in the equatorial limbs of 0.3 ± 0.1

We have insufficient resolution to determine the extent of the limb brightening in heliographic latitude except to say that the data is not well fit by restricting the

limb brightening to equal point sources on each limb. Earlier published observations, especially those of Christiansen and Warburton (1955), suggested that limb brightening is limited to the equatorial regions. Our value of the excess fractional flux in the limbs is higher than the 10% we estimated from the figure of Christiansen and Warburton (1955). However, they comment that the image needs to be corrected for smoothing and some of the flux contribution from the limbs is in the ellipticity of the image. We tested extending the limb emission beyond the optical limb of the Sun and could not improve our fits for an extension of up to 10% of the solar radius and beyond 10% extension the fits degraded rapidly.

A theoretical basis for limb brightening was given by Smerd (1950) assuming a spherically symmetric model of the solar atmosphere. It is now known from measurements of the Ulysses spacecraft (McComas et al. 2000) that the electron density in the solar atmosphere is more highly concentrated in the equatorial regions due to concentration by the Sun's magnetic field which is approximately aligned with the Sun's rotation axis.

To test a model based on solar physics we have used the expressions for the absorption and refractivity (Smerd's equations 3.13 through 3.17) combined with the electron density of Selhorst, Silva and Costa (2005) and temperature variation in the corona given by Gabriel (1992).

At our observing frequency of 1417 MHz the solar brightness temperature is dominated by absorption in the corona as the average brightness inferred from the measured flux density of $40 \pm 10 \times 10^{-22} \text{ WHz}^{-1} \text{ m}^{-2}$ is 10^5 K which is well above the temperature of the chromosphere. To produce an enhancement of the limb brightening in the equatorial regions we introduced a solar latitude dependence the electron density as indicated in the Ulysses spacecraft data given in figure 3 of McComas et al (2000). In order to produce a model with a reasonable fit our data we multiplied the densities given in table 1 of Selhorst, Silva and Costa (2005) by

$$16(1 - e^{-h/10^5})e^{-|lat|} + 0.6 \quad (2)$$

where lat is the latitude in radians and h is the height above the surface of the Sun in km. The expression above forces the electron density to become more spherically symmetric close to the chromosphere to avoid having the solar brightness fall off toward the poles across the entire solar disk.

In deriving the Sun model using ray tracing we accounted for a radial dependence of the electron temperature, T , using the integral

$$\int T(r) e^{-\tau(s)} ds \quad (3)$$

where the opacity, τ , is given by

$$\tau(s) = \int_0^s a(\ell) d\ell \quad (4)$$

where a is the absorption coefficient. We used Snell's law to modify the direction of each ray at the interface of each shell of constant refractivity in the computation. Figure 4 shows the model and the fit to the data of day 189 as an example. With the somewhat arbitrary latitude dependence given in equation 2 we found a model, based on the ray tracing, that fit the data almost as well as the empirical model of Figure 2. We note that the ray tracing model always produced some limb brightening in the polar regions. Selhorst, Silva and Costa (2005) required the addition of spicules extending into the corona to model the reduced polar limb brightening observed by the Nobeyama Radio Heliograph at 17 GHz. In general the ray trace model always produced more limb brightening than needed to fit the data.

The following table summarizes the quality of the fits to the solar images averaged over all the days for which we have data.

Quality of model fits

Model	Rms residual	Corona density and temperature model
Uniform disk	0.11	-
Disk with 30% equatorial limb brightening	0.05	-
Disk with 30% symmetric limb brightening	0.13	-
Best ray traced model	0.07	Selhorst, Silver, Costa (2005)
Best ray traced model	0.10	Newkirk (1961)

Note: All models included a single sunspot. We were able to improve the ray trace model to fit the data as well as the empirical model by artificially reducing

the limb brightening. Physically this could be accomplished by some scattering mechanism.

4. Conclusions

Data taken with a 3-element interferometer at 21 cm wavelength with short baselines shows clear evidence for limb brightening in the equatorial regions. Image models based on the corona density of Selhorst, Silva and Costa (2005) with an equatorial density enhancement suggested by the Ulysses data and the coronal temperature profile of Gabriel (1992) fit the data better than the older density profiles of the Newkirk (1961) model. The physical models without spicules or other scattering mechanism produce more limb brightening than the best fit model.

Acknowledgements

This work was supported by the national Science Foundation Research Experiences for Undergraduates (REU) program under grant AST-0138506. We thank the Haystack Observatory staff for their assistance in setting up the SRT interferometer.

References

- Christiansen, W.N., and Warburton, J.A., 1955, *Aust.*
- Gabriel, A.H. 1992 in the Sun, A laboratory for Astrophysics, ed. J.T. Schmelz & J.C. Brown, (Kluwer Academic Publishers) 277.
- McComas et al., 2000, *JGR*, 105, A5, 10, 419.
- Newkirk, G., 1961, *Ap.J.*, 133, 983.
- Roosen, J. and Goh, T., 1967, *Solar Physics*.
- Selhorst, C.L., Silva, A.V.R., & Costa, J.E.R., 2005, *A&A*, 433, 365.
- Smerd, S.F., 1950, *Aust. J. Sci. Res.*, A3, 34.



FIG. 1.- View of 3 small radio telescopes tracking the Sun in the parking lot of MIT Haystack Observatory at latitude 42.5°N 71.5°W .

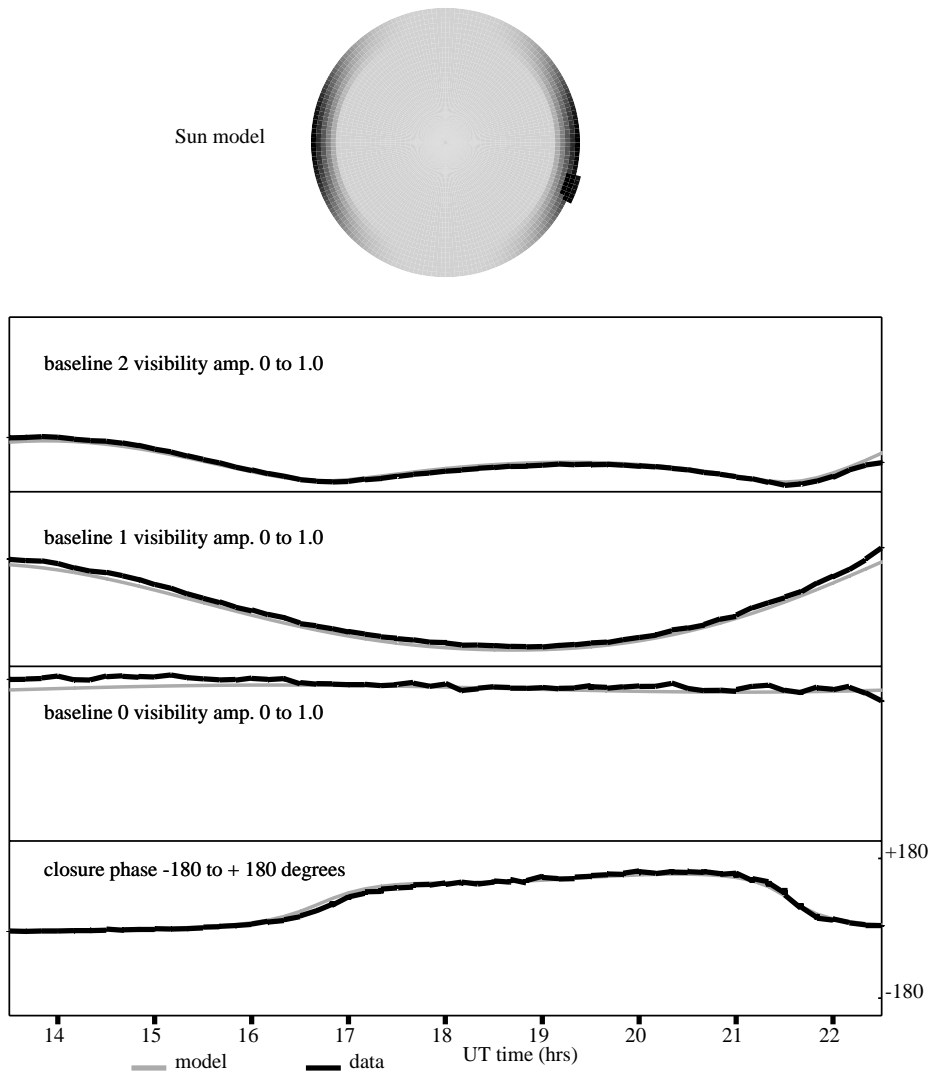


FIG. 2. – Best fit empirical model for 8 July 2006 (day number 189). The r.m.s. residual to the fit is 0.05. The fraction of flux in the limb is 26% of the total Sun’s total measured flux density of $40 \pm 10 \times 10^{-22} \text{ W Hz}^{-1} \text{ m}^{-2}$. The fraction of flux in the sunspot (NOAA active region AR898) located on the east limb is 7%. The average radio brightness for this day was approximately 10^5 K .

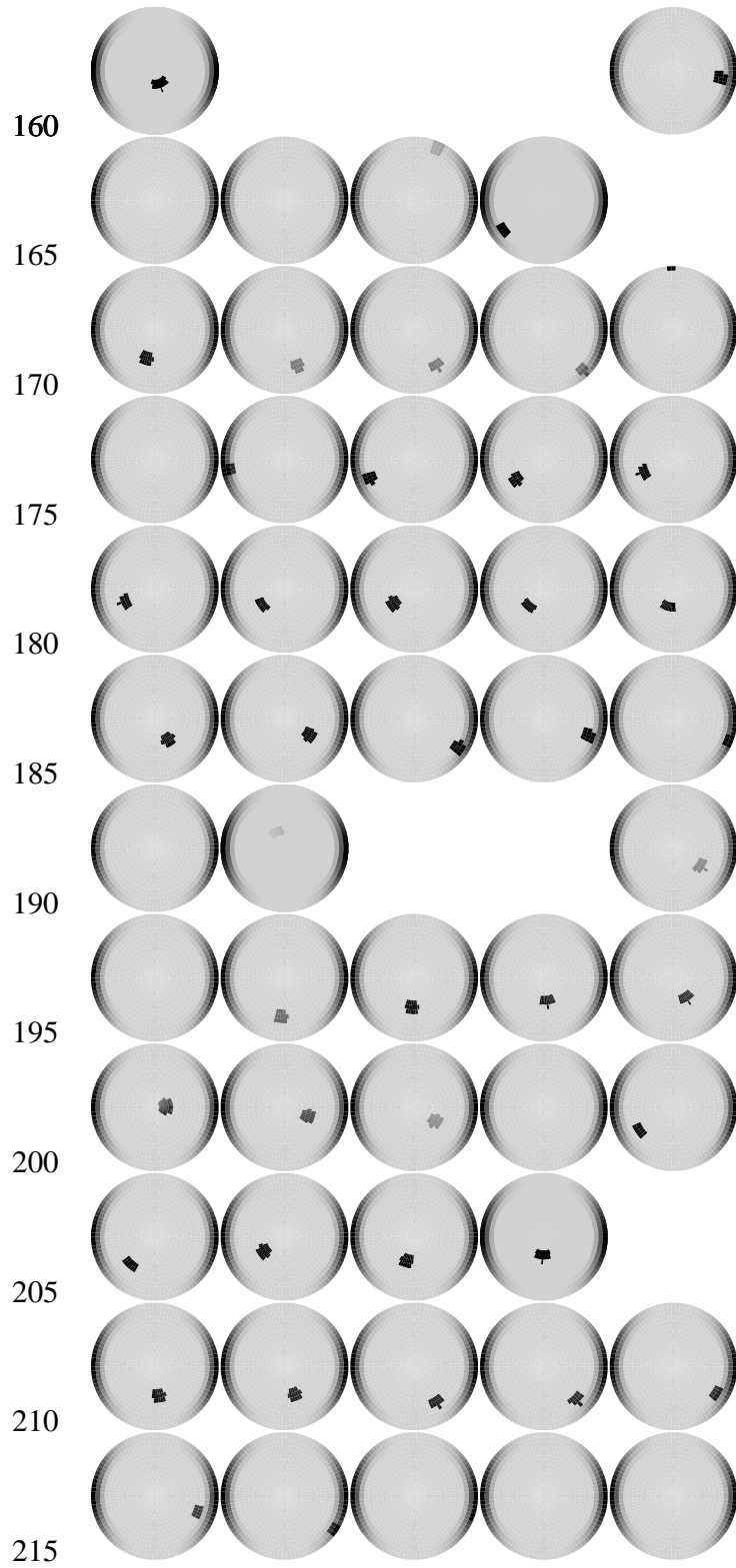


FIG. 3. – Sequence of best fit empirical models for days 160 through 219. Sunspot 898 (NOAA AR898) is seen to move across the disk from day 179 through 189.

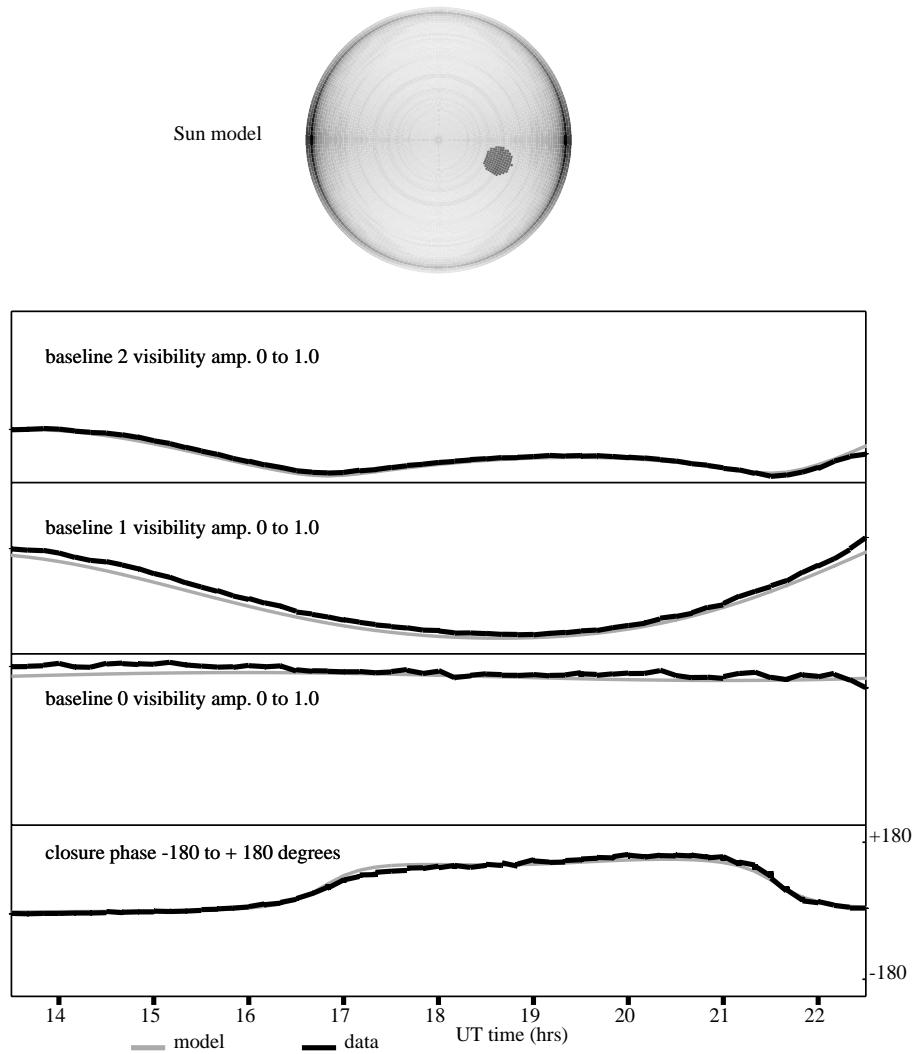


FIG. 4. – Best fit physical model for 2006. The physical model is based on ray tracing through the solar corona (see text). The r.m.s. residual to the fit is 0.07. The fraction of the flux in the limb is 34%. The fraction of flux in the sunspot is 7%. The fraction of flux in the limb is larger than the best fit empirical model and the sunspot location is displaced. Selhorst Silva and Costa (2005) suggest spicules in the corona as a mechanism for reducing the limb brightening.